

Modeling, and Dynamic control of DFIG with Integrated Battery Energy Storage System through LVRT Behavior

Jaya Raju Manepalli¹, G. Venkata Ratnam² Shaik Shaheem³

¹(Assistant prof. Electrical and Electronic Engineering, Avanti institute of engg. And tech., India)

²(Assistant prof. Electrical and Electronic Engineering, Avanti institute of engg. And tech., India)

³(Assistant prof. Electrical and Electronic Engineering, Avanti institute of engg. And tech., India)

Abstract: The Doubly Fed Induction Generator (DFIG) based wind turbine with variable-speed variable-pitch control scheme is the most popular wind power generator in the wind power industry. This machine can be operated either in grid connected or standalone mode. A thorough understanding of the modeling, control, and dynamic as well as the steady state analysis of this machine in both operation modes is necessary to optimally extract the power from the wind and accurately predict its performance. Which include Low Voltage Ride Through (LVRT) with Enhanced Flux Oriented Control (EFOC) in Rotor Side Converter (RSC) and enhance its dynamic behavior with integrated Battery Energy Storage System (BESS) at dc link capacitor. The theme of the paper is to improve the dynamic characteristics of the system

Keywords: Doubly Fed Induction Generator (DFIG); Battery Energy Storage System (BESS); Enhanced Flux Oriented Control (EFOC).

I. Introduction

In this thesis, a detailed electromechanical model of a DFIG-based wind turbine connected to power grid as well as autonomously operated wind turbine system with integrated battery energy storage is developed in the Matlab/Simulink environment and its corresponding generator and turbine control structure is implemented. A thorough explanation of this control structure as well as the steady state behaviour of the overall wind turbine system is presented. The steady state reactive power capability of the DFIG is studied

Doubly Fed Induction Generator (DFIG) offers low distortions in stator, rotor and grid currents due to closed loop control offered by back to back voltage source converter [3], as shown in Fig. 1 The present paper describes how LVRT behavior is achieved without sacrificing dynamic stability of DFIG system using an advanced control technique Enhanced Flux Oriented Control (EFOC) to reduce over currents along with aid of cost effective Battery Energy Storage System (BESS) connected through bidirectional switches to the dc link. This supports voltage at dc link and improves dynamic stability during symmetrical grid disturbances

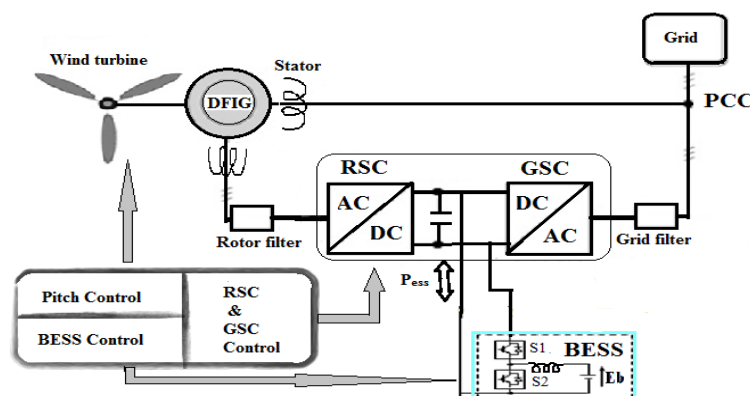


Fig. 1. BESS integrated wind turbine

II. Dynamic Modeling of DFIG

The vector control scheme of DFIG is done in a synchronously rotating reference frame to enable decoupled active and reactive power control and enhance sensibility of the system in improving dynamic response. The equivalent circuit of DFIG [10], [12] is as shown in Fig. 2, whose vector dynamics are independently shown in GSC and RSC control strategies

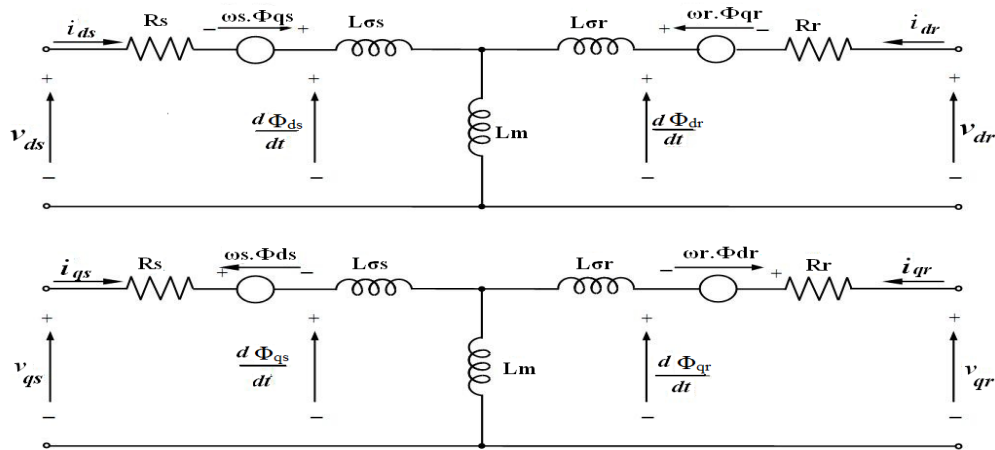


Fig. 2. Equivalent circuit of DFIG

$$V_{ds} = i_{ds}R_s - \omega_s\phi_{qs} + \frac{d}{dt}\phi_{ds} \tag{1}$$

$$V_{qs} = i_{qs}R_s - \omega_s\phi_{ds} + \frac{d}{dt}\phi_{qs} \tag{2}$$

Since the stator is directly connected to the grid, better current regulation can be employed by modifying the above equations (1) and (2) to (3) and (4), whose control technique [4] is shown in Fig. 3.

$$V_{dg} = (i_{dg}^* - i_{dg})R_s - \omega_s L_g i_{qg} + V_{ds} \tag{3}$$

$$V_{qg} = (i_{qg}^* - i_{qg})R_s - \omega_s L_g i_{dg} \tag{4}$$

where, $\frac{d\phi_{qs}}{dt} \cong 0$, Indicates non alignment of ϕ_{qs} with rotating stator flux.

Here the suffix ‘s’ refers to stator, replaced with ‘g’ refers to grid. The dependency of i_{dg} on dc capacitor voltage generates its reference i_{dg}^* . The reactive power exchange between GSC and Point of Common Coupling (PCC) is determined by i_{qg}^* [8] whose proportionalities are incorporated in PI controllers.

The decoupled control in GSC is achieved due to compensation offered by the cross coupling terms $-\omega_s L_g i_{qg}$, V_{ds} and $\omega_s L_g i_{dg}$, which are summed up to the output of PI regulators to avoid coupling effects.

A. Rotor Side Converter Control

RSC control achieves the stator active and reactive power control through i_{qr} and i_{dr} components respectively. The rotor voltage with respect to stationary reference frame [11] is given by

$$V_r^s = V_{0r}^s + (R_r i_r^s) + \sigma L_r \frac{di_r^s}{dt} - j\omega_i r^s \tag{5}$$

where, $\sigma = 1 - (\frac{L_m^2}{L_s L_r})$

V_{0r}^s , voltage induced due to stator flux

$$= \frac{L_m}{L_s} (\frac{d}{dt} - j\omega_s) \phi_s^s \tag{6}$$

$$\phi_s^s = L_s i_s^s + L_m i_r^s \tag{7}$$

$$\phi_r^s = L_r i_r^s + L_m i_s^s \tag{8}$$

The above equations (5), (7) and (8) in the synchronous rotating reference frame are given by

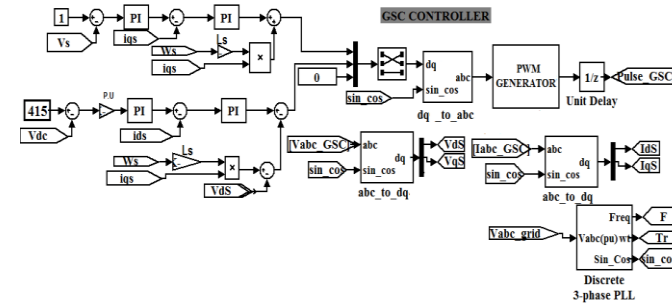


Fig. 3. GSC controller

$$V_{dr} = \frac{d\phi_{dr}}{dt} - (\omega_s - \omega)\phi_{qr} + R_r i_{dr} \tag{9}$$

$$V_{qr} = \frac{d\phi_{qr}}{dt} - (\omega_s - \omega)\phi_{dr} + R_r i_{qr} \tag{10}$$

$$\phi_{dr} = (L_{lr} + L_m)i_{dr} + L_m i_{ds} \tag{11}$$

$$\phi_{qr} = (L_{lr} + L_m)i_{qr} + L_m i_{qs} \tag{12}$$

$$\phi_{ds} = (L_{ls} + L_m)i_{ds} + L_m i_{dr} \tag{13}$$

$$\phi_{qs} = (L_{ls} + L_m)i_{qs} + L_m i_{qr} \tag{14}$$

where, $L_r = L_{lr} + L_m$

$$L_s = L_{ls} + L_m$$

$$\omega_r = \omega_s - \omega$$

By substituting (11), (12), (13), (14) in (9), (10) and by rearranging the terms, then

$$V_{dr} = (R_r + \frac{d}{dt} L'_r) i_{dr} - s\omega_s L_r i_{qr} + \frac{L_m}{L_s} V_{ds} \tag{15}$$

$$V_{qr} = (R_r + \frac{d}{dt} L'_r) i_{qr} + s\omega_s L_r i_{dr} + \frac{L_m}{L_s} (V_{qs} - \omega\phi_{ds}) \tag{16}$$

Where ω is rotor speed, ω_{ϕ_s} is speed of stator flux, ω_s is synchronous speed

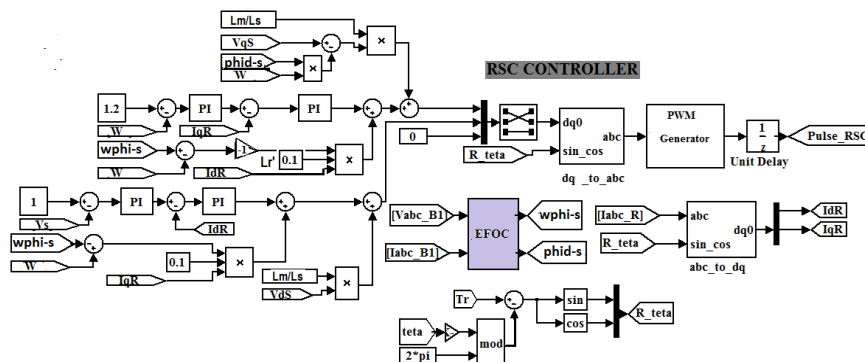


Fig. 4. RSC controller

1) Three Phase Symmetrical Faults

The stator voltage becomes zero during three phase symmetrical faults and stator flux ϕ_s also reduces to zero but with inertial time lag $\tau_s = \frac{L_s}{R_s}$ effecting rotor induced Electromotive Force (EMF) V_{or} . The flux during fault is given by

$$\phi_{sf}^s = \phi_s^s e^{-t/\tau_s} \tag{17}$$

and $\frac{d\phi_s^s}{dt}$ is negative, indicating its decay. By substituting (17) in (6)

$$V_{or}^s = -\frac{L_m}{L_s} \left(\frac{1}{\tau_s} + j\omega \right) \phi_s^s e^{-t/\tau_s} \tag{18}$$

Converting the above equation in the rotor reference frame and by neglecting $1/\tau_s$

$$V_{or}^r = -\frac{L_m}{L_s} (j\omega) \phi_s^s e^{-j\omega t} \tag{19}$$

$$|V_{or}^r| \propto |\phi_s^s| \tag{20}$$

By substituting $\phi_s^s = \frac{V_s^s}{j\omega_s} e^{j\omega_s t}$ in (19)

$$V_{or}^r = -\frac{L_m}{L_s} (1-s)V_s \tag{21}$$

$$|V_{or}^r| \propto (1-s) \tag{22}$$

Converting equation (5) into rotor reference frame

$$V_r^r = V_{or}^r e^{-j\omega t} + (R_r i_r^r) + \sigma L_r \frac{di_r^r}{dt} \tag{23}$$

Thus rotor equivalent circuit derived from (23) is as shown in Fig. 5 [11].

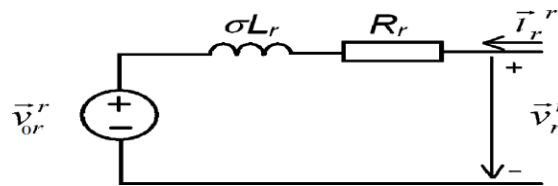


Fig. 5. The rotor equivalent circuit

It is to be noted that the considerable difference between V_r^r and V_{or}^r increase during three phase dip. Hence the RSC converter is rated high to enable the rotor voltage V_r^r to catch V_{or}^r for rotor current control. This voltage difference occurs due to increase in V_{or}^r and its reasons are listed below:

1. At first occurrence of fault ϕ_s does not falls instantly (20),
2. The machine running at super synchronous speed with slip approximately -0.25 increases the term $(1-s)$ (22).

The above factors are uncontrollable for a machine with high electrical and mechanical inertia. But to control rotor current, V_r^r can be increased. According to first reason listed above a voltage V_{ϕ_s} can be injected in the feed forward path. It is deduced as below:

Converting equation (19) into synchronous reference frame and by considering direct alignment of ϕ_{ds} with ϕ_s one can get,

$$V_{\phi_s} = \frac{-L_m}{L_s} \omega \phi_{ds} \tag{24}$$

The second reason listed above is compensated by replacing $s\omega_s$ with $(\omega_{\phi_s} - \omega)$ in cross coupling terms $s\omega_s L_r i_{qr}$ and $s\omega_s L_r i_{dr}$. The reduction in magnitude and frequency of flux ϕ_s , and alignment of flux with the stator voltage without rate of change in flux angle θ_{ϕ_s} indicate dc offset component in flux.

$$\frac{d\theta_{\phi_s}}{dt} = \omega_{\phi_s} - \omega = \omega_f \tag{25}$$

where, ω_f is the speed of stator flux during fault.

The voltage injection components (24) and compensating components discussed above are estimated with enhanced flux oriented scheme whose flow chart is shown in Fig. 6 and the determined values are incorporated in RSC controller shown in Fig. 4.

1) **Asymmetric Faults**

The same control technique can be employed for single phase to ground as well as two phase to ground faults. But due to presence of positive and negative sequence components, the rate of change in flux angle θ_{ϕ_s} and magnitude change in flux is observed [4], given by

$$\frac{d\theta_{\phi_s}}{dt} = \omega_{\phi_s} = \frac{(V_{\beta s} \phi_{\alpha s} - V_{\alpha s} \phi_{\beta s})}{(\phi_{\alpha s}^2 + \phi_{\beta s}^2)} = \omega_f \tag{26}$$

III. BESS Power Management

The Battery Energy Storage System supports the dc link capacitor during starting state and fault transient state of DFIG wind energy conversion system. The aiding process can be done accordingly with variations in active power P_{pcc} at point of common coupling to track the reference power P_{ref} generated with respect to wind speed V_w [15]. This variation in active power difference occurs during starting and fault conditions, resulting in an extra power. Hence this excess power P_{ex} is allowed to pass through the bypass link provided by RSC and GSC controllers via dc link capacitor

According to DFIG starting characteristics [10], [12] the capacitor should maintain sufficient initial charge, for this BESS offers its help with initial state of charge (SOC) 51%. During severe faults, the battery aids the dc link through the action of bidirectional switches (IGBT diodes) connected via inductor. The control signals to IGBT diodes depend on the active power difference between P_{pcc} and P_{ref} which generates reference battery current. Such that the battery current is regulated is shown in Fig. 7

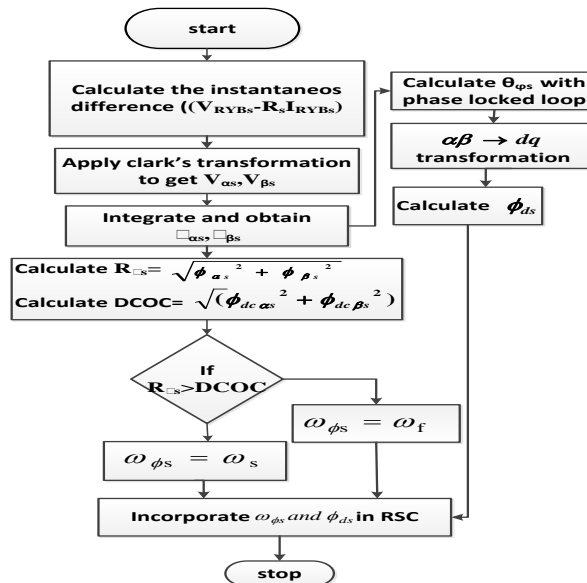


Fig. 6. Scheme of enhanced flux oriented control

where, DCOC=dc offset component of flux, R_{ϕ_s} =radius of flux trajectory.

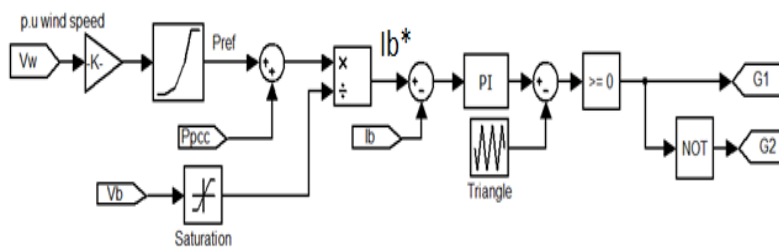


Fig. 7. BESS control

However, BESS provides efficient support to the system under severe faults by controlling real and reactive power flows to the grid maintaining constant dc link voltage particularly during transient state. Thus improves dynamic stability of the system

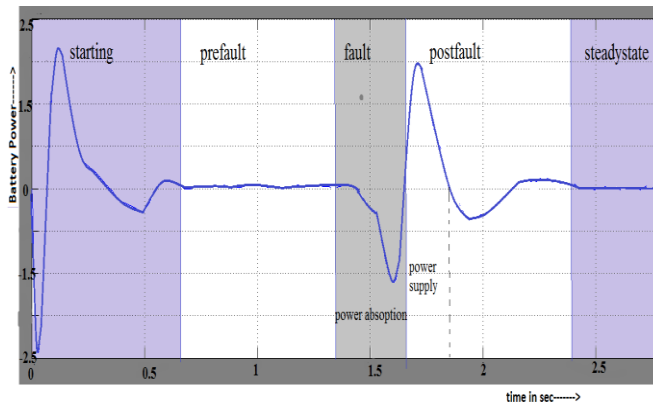


Fig. 8. Power management characteristics of BESS

IV. Pitch Angle Control

The pitch angle of the wind turbine can be controlled to protect the wind turbine from high speed and also provide sufficient mechanical torque even at low speed for active power control at the grid. It allows the wind turbine to track rotor reference speed and compensation is allowed through active power difference between P_{ref1} and P_{ref2} . Where, P_{ref1} is derived from power at PCC assuming 10% losses and P_{ref2} is derived according to wind speed V_w . The Pitch angle control circuit is shown in Fig. 9.

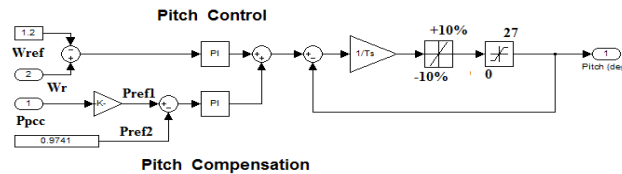
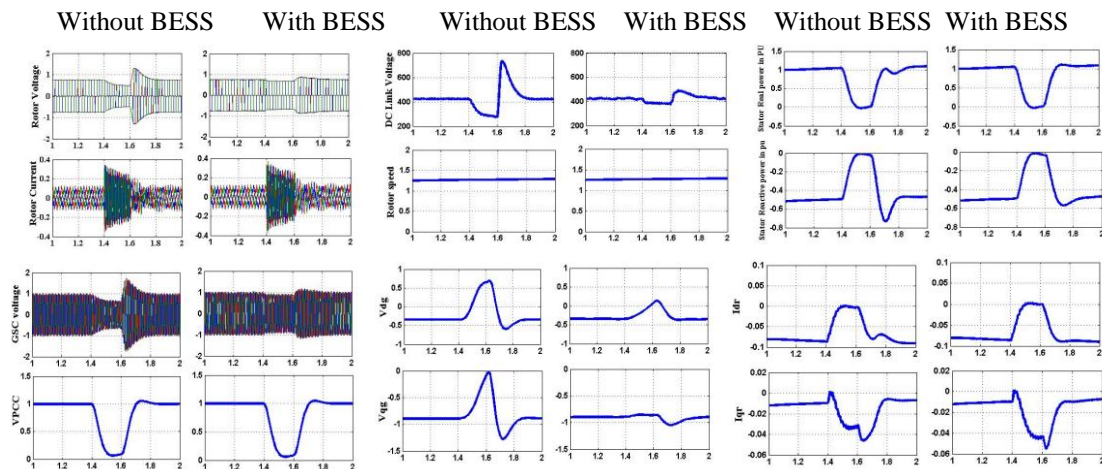
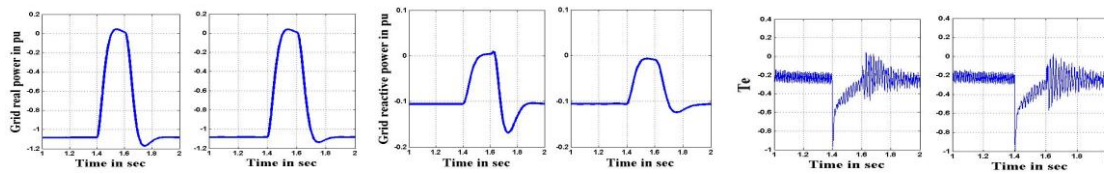


Fig. 9. Pitch angle control

V.Result Analysis

According to Nordiac wind grid code, during symmetrical three phase faults, the wind power system should resume its normal operation within 50msec of time even though the voltage sags to zero percent. In the present system for fault duration of 0.2 sec, LVRT behavior and control of abnormal rotor current is achieved with efficient EFOC control scheme instead of conventional techniques. In addition to LVRT behavior, the dynamic response is improved with the help of cost effective BESS rated at a nominal voltage of 400V, with rated capacity of 2.5 ampere-hour, for a dc link voltage of 415V





Achieving LVRT behavior is difficult in super synchronous mode hence the RSC voltage is rated high to 34.5KV and wind speed is assumed to be 14 m/sec

VI. Conclusion

The wind energy conversion system is said to be good enough when it provides good quality of power. It can be achieved by a system with good LVRT capacity ensuring dynamic stability by obeying wind grid codes. The present system offers its LVRT capability according to NORDIAC wind grid code. Also it mitigates transient over currents in rotor circuit by using advanced EFOC algorithmic technique. Thus, avoids usage of crowbar circuit which throws the grid into more vulnerable situation by demanding reactive power.

The overall dynamic response of the system is improved by suppressing fault and post fault transients enhancing the lethargic system to reach its steady state at an improved rate, thus providing good quality as well as reliable power with the aid of BESS.

The novelty of the proposed technique is proved with help of MATLAB/SIMULINK tool which shows the effectiveness of EFOC technique and a comparison between with and without BESS in all aspects of real and reactive powers, direct and quadrature components of rotor current, dc link capacitor voltage, rotor speed and electromagnetic torque during and after three phase symmetrical and asymmetrical faults. When cost is not of major concern, the future extension of this work can be made with super conducting magnetic energy storage [20] or fuel cell instead of battery energy storage system. Artificial intelligence techniques such as fuzzy logics or neural networks may be employed in calculating reference powers for precise control.

Appendix

The parameters of DFIG used in simulation are, Rated Power = 1.5MW, Rated Voltage = 690V, Stator Resistance $R_s = 0.0049pu$, rotor Resistance $R_r = 0.0049pu$, Stator Leakage Inductance $L_{ls} = 0.093pu$, Rotor Leakage inductance $L_{lr} = 0.1pu$, Inertia constant = 4.54pu, Number of poles = 4, Mutual Inductance $L_m = 3.39 pu$, DC link Voltage = 415V, Dc link capacitance = 0.2F, Wind speed = 14 m/sec. Grid Voltage = 25 KV, Grid frequency = 60 Hz. Grid side Filter: $R_{fg} = 0.3\Omega$, $L_{fg} = 0.6nH$ Rotor side filter: $R_{fr} = 0.3m\Omega$, $L_{fr} = 0.6nH$

References

- [1]. Nordel, "Nordic grid code," January 2007.
- [2]. <http://www.bwea.com/edu/wind.html>.
- [3]. Sarasij Das, Ramesh Pampana, "Draft report on Indian Wind Grid Code" submitted to Centre for Wind Energy Technology, Tamilnadu, India, July 2009.
- [4]. Joshi. N, Mohan. N, "A Novel Scheme to Connect Wind Turbines to the Power Grid," *IEEE Trans. Energy Conversion*, vol.24, no.2, pp. 504-510, June 2009.
- [5]. Jiaqi Liang, Wei Qiao, Harley. R.G, "Feed-Forward Transient Current Control for Low-Voltage Ride-Through Enhancement of DFIG Wind Turbines," *IEEE Trans. Energy Conversion*, vol.25, no.3, pp. 836-843, Sept 2010.
- [6]. Lixin Ma, Yiwen Zheng, Heran Ma, "Research and simulation of double-fed wind power generation rotor side control technology," *Electrical and Control Engineering (ICECE), 2011 International Conference*, pp. 2472-2475, Sept 2011.
- [7]. Sylvain .L. S, "Voltage Oriented Control of Three-Phase Boost PWM Converters," M.S. thesis, Dept. Elec. Power Eng., Chalmers Univ. of Tech., Goteborg, Sweden, 2010.
- [8]. Bijaya Pokharel, "Modeling, Control and Analysis of a Doubly Fed Induction Generator Based Wind Turbine System with Voltage Regulation," M.S. thesis, Dept. Elec. Eng., Tennessee Tech. Univ., Cookeville, Tennessee, Dec 2011.
- [9]. Liyan Qu, Wei Qiao, "Constant Power Control of DFIG Wind Turbines With Super capacitor Energy Storage," *IEEE Trans. Industry Applications*, vol. 47, pp. 359-367, Feb 2011.
- [10]. Chad Abbey, "A Doubly Fed Induction Generator And Energy Storage System For Wind Power Applications," M.E. thesis, Dept. Elec. and Comp. Eng., Alberta Univ., Edmonton, Alberta.
- [11]. Amarendra Edpuganti, "Low Voltage Ride Through Solutions for DFIG Wind Turbine," M.Tech. thesis, Dept. Elec. Eng., IIT Kanpur, Kanpur, India.
- [12]. Lopez. J, Sanchis. P, Roboam. X, Marroyo. L, "Dynamic Behavior of the Doubly Fed Induction Generator During Three-Phase Voltage Dips," *IEEE Trans. Energy Conversion*, vol. 22, pp. 709-717, Sept. 2007.
- [13]. G. Abad, J. Lopez, L. Marroyo, M. Rodriguez, and G. Iwanski, "Doubly Fed Induction Machine: Modelling and Control for Wind Energy Generation Applications," *IEEE Press Series on Power Eng.*, John Wiley & Sons, 2011.
- [14]. Irtaza M. S, Bala Venkatesh, Bin Wu, Alexandre B. N, "Two-layer control scheme for a Super capacitor Energy Storage System coupled to a Doubly Fed Induction Generator," *ELSEVIER, Electrical Power Systems Research* 86, 2012, pp. 76-83.
- [15]. S. M. Muyeen, Rion Takahashi, Toshiaki Murata, Junji Tamura, Mohd. Hasan Ali, "Application of STATCOM/BESS for wind power smoothening and hydrogen generation" *ELSEVIER, Electrical Power Systems Research* 79, 2009, pp. 365-373.
- [16]. Okedu. K.E, Muyeen. S. M, Takahashi. R, Tamura. J, "Comparative study of wind farm stabilization using variable speed generator and FACTS device," *GCC Conference and Exhibition (GCC), 2011 IEEE*, pp. 569-572, Feb 2011.

- [17]. Johan Morren, Sjoerd W. H. de Haan, "Ride through of Wind Turbines with Doubly-Fed Induction Generator During a Voltage Dip," *IEEE Trans. Energy Conversion*, vol. 20, pp. 435-441, June 2005.
- [18]. Seman. S, Niiranen. J, Arkkio. A, "Ride-Through Analysis of Doubly Fed Induction Wind-Power Generator Under Unsymmetrical Network Disturbance," *IEEE Trans. Power Systems*, vol. 21, pp.1782-1789, Nov 2006.
- [19]. Erlich. I, Wrede. H, Feltes. C, "Dynamic Behavior of DFIG-Based Wind Turbines during Grid Faults," *Power Conversion Conference - Nagoya, 2007. PCC '07*, pp. 1195-1200, April 2007.
- [20]. Pannell. G, Zahawi. B, Atkinson. D. J, Missailidis. P, "Evaluation of the Performance of a DC-Link Brake Chopper as a DFIG Low-Voltage Fault-Ride-Through Device," *IEEE Trans. Energy Conversion*, pp. 1-8, May 2013.
- [21]. Pal. B. C. Coonick. A. H. Macdonald, Donald. C, "Robust Damping Controller Design In Power Systems With Superconducting Magnetic Energy Storage Devices," *IEEE Trans. Power Systems*, vol. 15, pp. 320-325, Feb 2000.